J Mol Model (2013) 19:2107–2118
DOI 10.1007/s00894-012-1631-9

ORIGINAL PAPER

Ethylene dimerization catalyzed by mixed phosphine–iminophosphorane nickel(II) complexes: a DFT investigation

Vincent Tognetti · Antoine Buchard · Audrey Auffrant · Ilaria Ciofini · Pascal Le Floch · Carlo Adamo

Received: 19 April 2012 / Accepted: 5 October 2012 / Published online: 28 November 2012

Abstract A computational study utilizing density functional theory (DFT) was performed to analyze the mechanism of ethylene dimerization catalyzed by (P,N) nickel(II) complexes, where (P,N) is a mixed phosphine–iminophosphorane ligand. Two plausible reaction pathways were considered, namely the Cossee and metallacycle pathways, for three model systems. The fundamental role of ligand assymetry and the importance of steric and *trans* effects were elucidated. In order to discriminate between both mechanisms, the activation of the precatalyst by trimethylaluminum was modeled. The results obtained allow the establishment of useful guidelines for creating new specifically tailored nickel-based catalysts for controlled dimerization.

Keywords Theoretical chemistry · DFT · Homogeneous catalysis · Reaction mechanism · Ethylene dimerization · (P,N) nickel(II) catalysts

The author Pascal Le Floch is now deceased.

V. Tognetti · I. Ciofini · C. Adamo (✉)
Laboratoire d'Electrochimie, Chimie des Interfaces et Modélisation pour l'Energie, LECIME CNRS UMR-7575, Ecole Nationale Supérieure de Chimie de Paris-Chimie ParisTech,
11 rue P. et M. Curie,
75231 Paris Cedex 05, Paris, France
e-mail: carlo-adamo@chimie-paristech.fr

A. Buchard · A. Auffrant · P. Le Floch
Ecole Polytechnique, CNRS,
Laboratoire "Hétéroéléments et Coordination",
91128 Palaiseau Cedex, France

Present Address:
V. Tognetti
COBRA IRCOF, CNRS UMR 6014 & FR 3038,
Université de Rouen et INSA de Rouen,
76821 Mont St Aignan Cedex, France

Introduction

Short-chain α-olefins are strategic targets in industrial chemistry, where they are used mainly as comonomers in the synthesis of low-density polyethylene [1]. Among them, C_4, C_6, and C_8 α-olefins are the most valuable compounds in terms of applications [2]. The oligomerization of ethylene is one of the easiest ways to produce these olefins. Titanium-based Ziegler–Natta systems [3] are the most widespread of the catalysts currently used to perform such transformations, but some alternative approaches using other transition metals have also been investigated over the last decade. For instance, chromium-based catalysts play a major role in ethylene tri- and tetramerization reactions [4–12]. It is worth noting that hexenes can be produced by propene dimerization catalyzed by either cobalt [13] or nickel [14] complexes. Importantly, these latter nickel complexes have shown very good catalytic activity in ethylene dimerization [15–17]. In this context, some of us have recently reported on the use of very efficient nickel(II) catalysts [18] based on mixed bidentate (P,N) ligands featuring both a phosphine and an imininophosphorane moiety [19, 20]. This catalytic system presents some notable advantages, such as availability, good stability, and excellent activity (more than 90 % 1-butene and turnover frequencies of >60,000 $mol_{C2H4}\ mol_{Ni}^{-1}\ h^{-1}$).

These very promising experimental results called for a detailed mechanistic study, since a better and more precise

understanding of the reaction process would enable the catalytic systems to be improved and permit the rational design of new active systems.

In this context, density functional theory (DFT) [21, 22] has become one of the major tools of quantum chemistry, due mainly to its reliability, low computational cost, and wide range of applications. Such approaches have been successfully applied to study a large number of catalytic transformations for over 20 years (see [23, 24] for examples), but the overall mechanism of transition metal catalyzed ethylene dimerization has not been studied using DFT; rather, they have focused on just one of the key steps in possible mechanisms [25–27].

Two main mechanisms should be considered for the oligomerization of ethylene. The first is the traditional Cossee mechanism [28], which involves a series of insertions (propagation step) of ethylene into a growing alkyl chain and a termination step in which a β-hydrogen transfer produces the final olefins (see Scheme 1a). In this mechanism, which has been extensively studied and reported in the literature, the formal oxidation state of the metal remains unchanged during the propagation step. Notably, this is the mechanism associated with Ziegler–Natta catalysis [29] and diimine complexes (containing palladium, nickel, iron, or cobalt centers [30–33]).

A second possible mechanism is the so-called metallacycle pathway, which begins with an oxidative coupling of two ethylene molecules to form a metallacyclopentane. The cycle can then be enlarged through successive ethylene insertions (see Scheme 1b). This mechanism is thought to occur in chromium-based systems such as the Phillips and Sasol processes [34, 35].

In the work described in this paper, these two possible reaction pathways were studied in detail, and the fundamental role played by the ligand in the catalyst coordination sphere was investigated.

In order to better understand the origin of the observed selectivity and the importance of the ligand substituents, calculations were performed on three model complexes differing by the substituents on the nitrogen and phosphorus atoms (see Fig. 1).

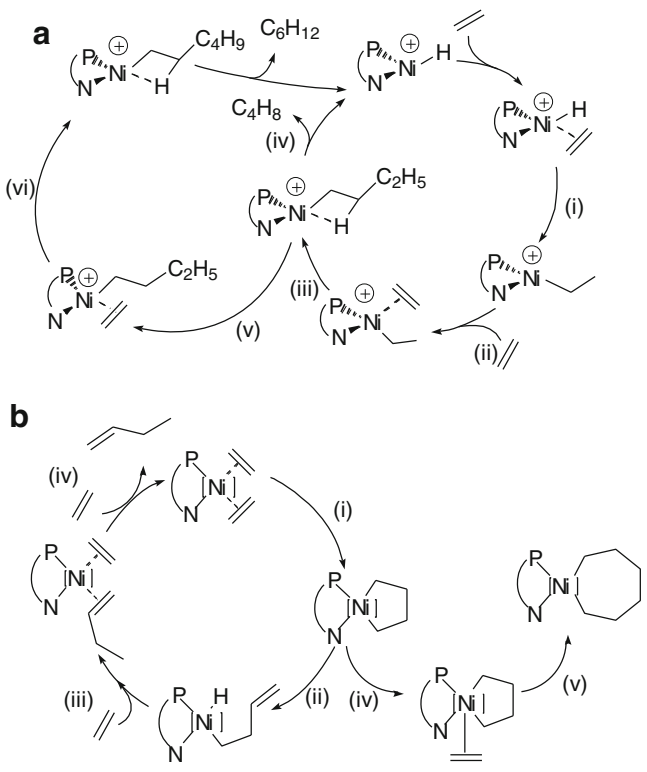

Scheme 1 Sketches of the Cossee (**a**) and metallacycle (**b**) mechanisms

Computational details

All calculations were carried out using the Gaussian 03 software suite [36] with the hybrid B3PW91 functional [37]. This functional has been extensively and successfully used in organometallic catalysis for many years (see for instance [38, 39]). The 6–31 G* basis set was used for all nonmetallic atoms (H, C, P, N), and the double-ζ quality basis designed by Hay and Wadt was employed in conjunction with its effective core potential for the nickel atom [40].

In the light of recent interesting studies on agostic complexes, one may wonder if polarization functions on hydrogen atoms are crucial to achieving accurate results [41–43]. To this end, we have reoptimized some agostic complexes (with the H substituents on N and P atoms) using the larger 6–31 G(d,p) basis set. The obtained results show, for instance, that the Gibbs energy difference between compounds **3a** and **4b** (agostic) is 19.4 kcal mol^{-1} with 6–31 G (d) and 19.6 kcal mol^{-1} with 6–31 G(d,p). Similarly, the difference between **5b** and **6a** is 14.7 (kcal mol^{-1}) and 15.0 kcal mol^{-1} with the same two basis sets. The same qualitative conclusions regarding geometries still hold, whichever basis set is employed. For instance, the M–H_β agostic bond lengths are equal to 1.73 A and 1.65 A in **4b** and **6a** with the 6–31 G* basis set, while they are 1.70 A and 1.63 A with 6–31 G**. It can therefore be safely assumed that these polarization functions on hydrogen atoms do not significantly affect the results, so all of the computations reported subsequently were carried out with the smaller 6–31 G(d) basis.

All structures were fully optimized and the nature of the stationary points was checked by analytically computing the Hessian matrix. In order to verify that the products and the reactants were correctly connected, intrinsic reaction coordinate (IRC) calculations [44, 45] were performed.

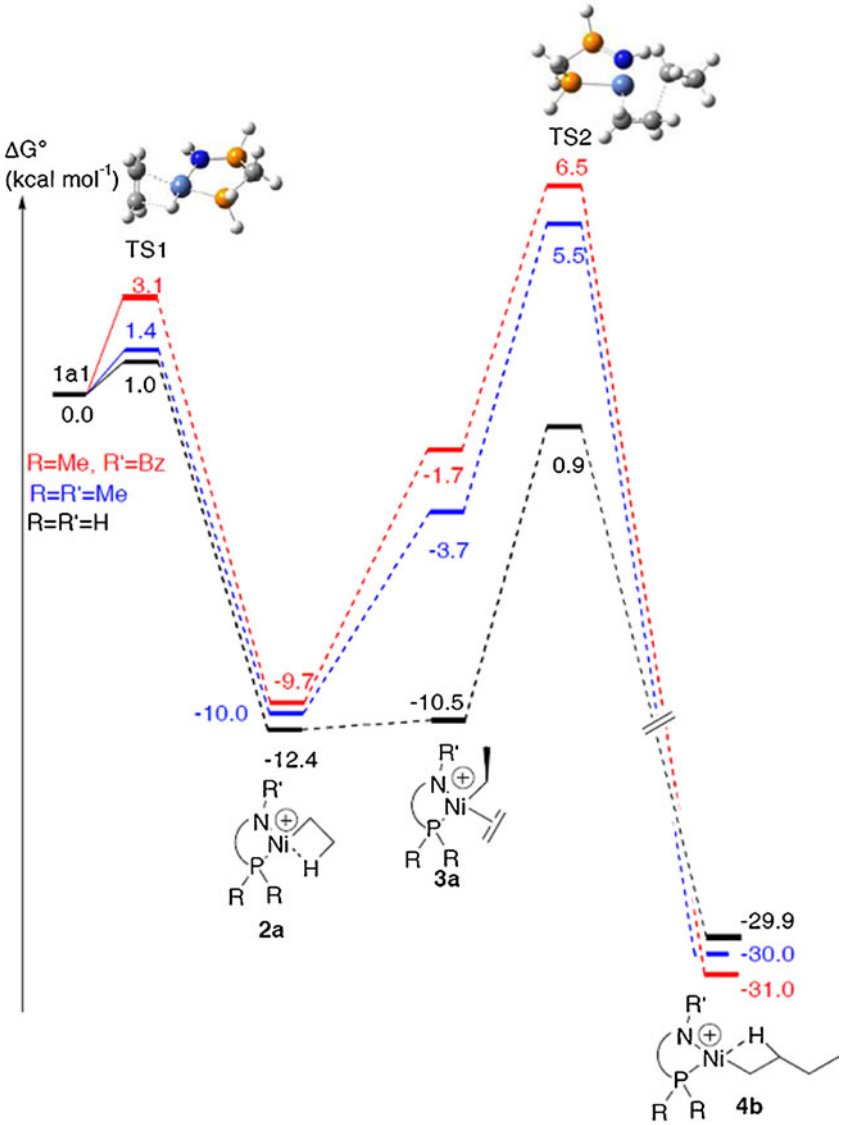

Fig. 1 Thermodynamics of the first two ethylene insertions (*orange* P, *gray* C, *white* H, *dark blue* N, *light blue* Ni)

Results and discussion

Cossee mechanism

Determination of the most stable spin states and conformers of the starting complexes

In the Cossee mechanism, the first step is the insertion of a previously coordinated ethylene molecule into a metal–hydride bond [46]. The formation of this hydride results from the activation of the precatalyst by the co-catalyst used in the experience [47]. The co-catalyst, for instance the very popular methylaluminoxane (MAO) [48], transfers a methyl group to the metal after the abstraction of halides in the precursor complex. Such a hypothesis was corroborated by the experiences of Brookhart and co-workers [49]. An ethylene molecule then inserts into the metal–carbon bond, and β-elimination of propene creates the metal–hydride bond [50]. For some systems, propene elimination does not occur and polymerization continues. Since only oligomers with an even number of carbon atoms were obtained with the studied catalysts, the first insertion is made into a metal–hydride bond and not into a metal–carbon one. These observations prompted us to consider as a starting precursor a hydride complex bearing the asymmetric bidentate (P,N) ligand and one molecule of ethylene.

Whatever the nature of substituents on the phosphorus or nitrogen atoms, singlet conformers were found to be considerably more stable than the corresponding triplet complexes (more than 13 kcal mol^{-1} higher), with the relationship between geometries (square planar or tetrahedral) and spin states (singlet or triplet, respectively) conforming to traditional molecular orbital theory for transition metal complexes.

Furthermore, the singlet complexes (denoted **1a1**) with the hydride located *trans* to the nitrogen atom are more

stable (by at least 5.9 kcal mol^{-1}) than the corresponding *cis* isomers. This (strong) *trans* effect increases with the hindrance at the nitrogen atom, so that only the *trans* system will be considered in the following calculations.

The first two insertions

The first insertion results from the rotation of the ethylene moiety, which is originally perpendicular to the mean coordination plane. As expected, this step does not require much energy (less than 3.1 kcal mol^{-1}, Fig. 1). The subsequent complex **2a** shows a β-agostic bond, which saturates the coordination sphere of the square-planar metal center, preventing any reversal of the insertion. The next step destabilizes the complex (by 8 kcal mol^{-1} at most), as a relatively strong interaction (the β-agostic one) is replaced with a weaker one (the π-interaction with ethylene). Indeed, the backdonation from the metal to the ethylene is rather weak, as shown by the C=C bond length in all **3a** complexes (1.38 Å).

Complexes **3a** then undergo an insertion, leading to a butyl chain with a β-agostic hydrogen. The activation barrier for this transformation is relatively low (about 10 kcal mol^{-1}) and depends only slightly on the nature of the N substituent. The energy of **4b** is independent of the N substituent; this can be explained by the position of the whole alkyl chain, which is located *trans* to the nitrogen atom, so that no interaction can develop between this substituent (even if it is bulky) and the growing chain. The stabilization induced by the agostic interaction makes the formation of **4b** very favorable from a thermodynamic point of view (30 kcal mol^{-1} below the energy of **1a1** and more than 20 kcal mol^{-1} below that of **2a**).

Third insertion and butene elimination

Competition between the third insertion (leading to the hexyl chain) and 1-butene elimination is the key factor governing the selectivity of the process (Fig. 2).[1] The third insertion implies the coordination of an additional ethylene molecule and consequently the loss of the agostic interaction. Again, this step is unfavorable, and—in contrast with the results given in the previous paragraph—it depends on the substituents (due to the position of the incoming ethylene molecule, which is now on the same side as the nitrogen group, potentially leading to steric interactions with it).

The selectivity for 1-butene vs superior oligomers can be rationalized in term of the energy difference between the two transition states:

$$\Delta G^0_{\mathrm{pref}} = \Delta G^0(\mathrm{TS3}) - \Delta G^0(\mathrm{TS4}). \quad (1)$$

Using this definition, $\Delta G^0_{\mathrm{pref}} > 0$ indicates that the insertion of an additional ethylene molecule is favored, whereas $\Delta G^0_{\mathrm{pref}} < 0$ implies that the elimination of 1-butene is preferred. In the R = R′ = H case, the computed $\Delta G^0_{\mathrm{pref}}$ is 0.8 kcal mol^{-1}, thus predicting that alkyl chain growth is more probable. On the contrary, $\Delta G^0_{\mathrm{pref}}$ is computed to be −2.7 kcal mol^{-1} and −5.6 kcal mol^{-1} when R = R′ = Me and R = Me, R′ = Bz, respectively, in agreement with the experimentally observed selectivity.

The key to understanding the efficiency of the process is to note that the insertion process is in fact the sum of two steps: the coordination of an ethylene molecule and the insertion itself. Neither of these steps requires much energy (around 13 kcal mol^{-1} and 17 kcal mol^{-1}, respectively), and each of these energies is smaller than the elimination barrier (23 kcal mol^{-1}): the butene selectivity stems from their sum. As the competition between agosticity vs p-interaction represents half of the energy of this process, the selectivity for butene is improved by increasing the steric hindrance at the nitrogen atom.

However, to be thorough, we should also consider another reaction pathway: β-hydrogen transfer (BHT). This transfer has been shown to be the main path in Ziegler–Natta reactions when using electron-deficient metal complexes (such as titanium, zirconium, or hafnium complexes) as catalysts [51, 52]. On the contrary, BHT does not occur with electron-rich transition metal complexes such as cobalt complexes. [53]

This mechanism can be viewed as the transfer of a β-hydrogen of the alkyl chain to the coordinated ethylene ligand (complex **5b**), leading to a metal center linked to an ethyl chain and to a π-coordinated 1-butene, which can in turn leave the coordination sphere (Fig. 3).

The computed activation barriers are, however, definitely prohibitive. A rather reasonable conjecture is that hydrogen–chain transfers are predominant for electron-poor metals whereas hydrogen–metal transfers dominate for electron-rich metals like nickel.

Hexene elimination

The last experimental fact to account for is that a significant amount of hexene is observed but none of the longer oligomers are detected. Figure 3 offers a rather simple

[1] Note that the reported transition state for elimination is the one associated with hydrogen transfer to the metal, which is the first step in butene elimination. The second step involves the release of butene by replacing the still-coordinated C_4H_8 with a C_2H_4 molecule. This step could only be modeled by a dynamic approach, so the point at −18.8 kcal mol^{-1} on the butene elimination path is obviously not meaningful and erroneously suggests that this elimination is reversible. However, as the ethylene is maintained at a high pressure (30 bars), the probability of another C_4H_8 coordinating is almost null.

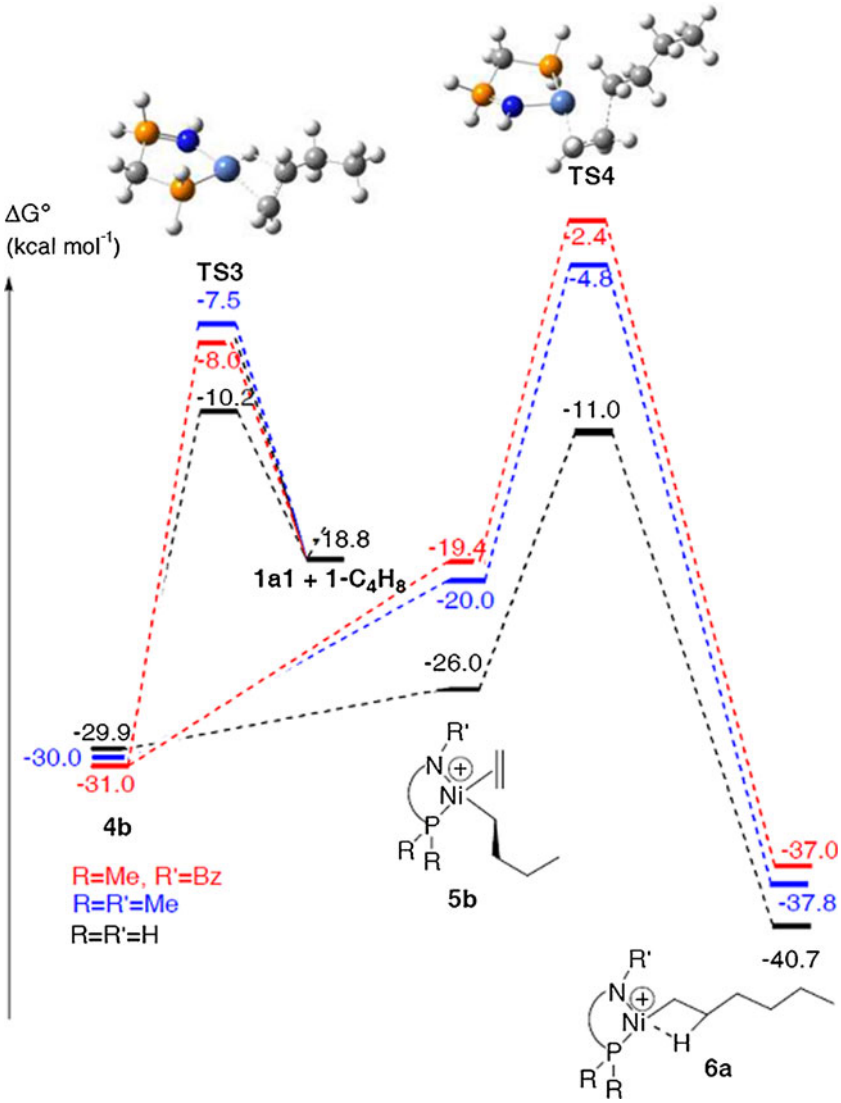

Fig. 2 Competition between the third insertion and butene elimination (*orange* P, *gray* C, *white* H, *dark blue* N, *light blue* Ni)

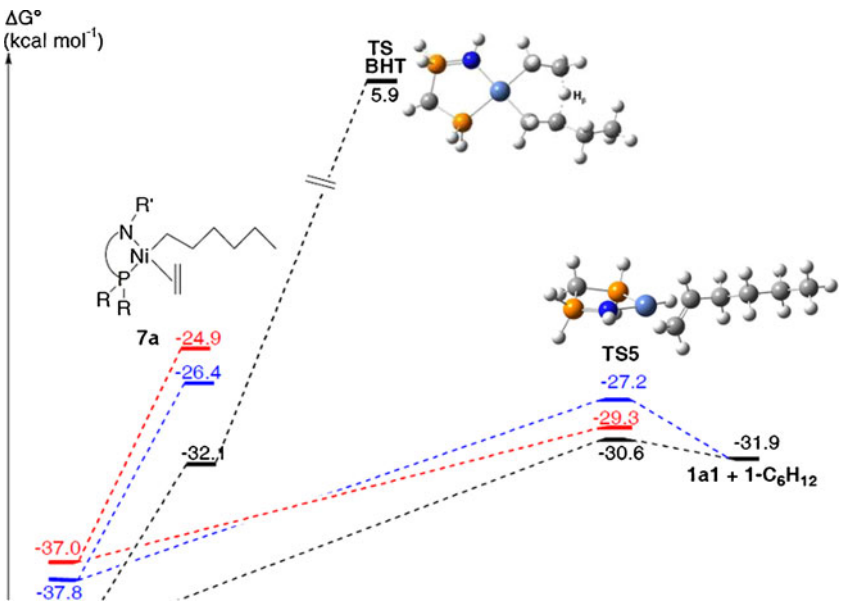

Fig. 3 Competition between the fourth insertion, β-hydrogen transfer, and hexene elimination (*orange* P, *gray* C, *white* H, *dark blue* N, *light blue* Ni)

explanation: complex **7a** is higher in energy than the transition state for hexene release. There is therefore no need to compute the fourth ethylene insertion to conclude that octene will not be detected.

Factors determining the selectivity

The results obtained up to now suggest that there are three main factors determining the observed selectivity in the case of the Cossee mechanism: the β-agostic interaction, the *trans* effect, and the steric hindrance at the nitrogen atom.

The stabilization brought about by the presence of the β-agostic interaction accounts for the selectivity in 1-butene, since it induces an energetic cost of coordinating an additional ethylene. This stabilization energy (ΔG°_{ago}, the energy difference between the nonagostic and the agostic complexes for the same chain length) increases with steric hindrance (see Table 1).

As the ligand is not symmetric, the possibility of coordinating an ethylene molecule to the metal depends on the atom located *trans* to the vacant coordination site: *trans* to the nitrogen (labeled "a") or *trans* to the phosphorus (labeled "b"). Thus, the stabilization or destabilization induced by the coordination of an ethylene molecule, depending on the site at which it occurs, can be computed as the difference in the energies required for the coordination either *trans* to the phosphorus ($\Delta G^{0}_{2b\rightarrow 3b}$) or *trans* to the nitrogen atom ($\Delta G^{0}_{2a\rightarrow 3a}$):

$$t^{0}_{2\rightarrow 3} = \Delta G^{0}_{2b\rightarrow 3b} - \Delta G^{0}_{2a\rightarrow 3a} \quad (2)$$

In this notation, $t^{0}_{2\rightarrow 3} > 0$ implies easier coordination of ethylene *trans* to N than *trans* to P, whereas $t^{0}_{2\rightarrow 3}$ indicates more difficult coordination *trans* to N. In a similar manner, the energy difference $t^{0}_{4\rightarrow 5}$ can be used to evaluate the *trans* preference for the transformation of complex **4** into complex **5**.

As all $t^{0}_{2\rightarrow 3}$ and $t^{0}_{4\rightarrow 5}$ values (Table 1) are positive, the coordination of an ethylene molecule *trans* to the phosphorus atom is always disfavored.

The *trans* effect is also enhanced by steric hindrance. This preference for the nitrogen atom is another clue to the 1-butene selectivity. Indeed, if we assume that the departure point is the most stable conformer **1a1**, the coordination of the second ethylene occurs *trans* to the nitrogen atom, i.e., the most favorable position. As a consequence, the third ethylene has to coordinate *trans* to P, which is the most unfavorable position, so the construction of the *n*-hexyl chain is disfavored. On the contrary, if the other conformer had been the most stable initial hydride complex, the coordination of the third ethylene would have occurred in the best position (*trans* to N) and the destabilization would have been weaker.

This *trans* effect can also be understood by studying the lengthening of the Ni–N bond length d^{Ni-N} with ethylene coordination. The quantities t^{Ni-N} compare the amount of partial decoordination when ethylene is *trans* to P with that when it is *trans* to N:

$$t^{Ni-N}_{2\rightarrow 3} = \left(d^{Ni-N}_{3b} - d^{Ni-N}_{2b}\right) - \left(d^{Ni-N}_{3a} - d^{Ni-N}_{2a}\right). \quad (3)$$

All calculated values (Table 1) are positive, indicating that the nitrogen atom moves away more when ethylene is *trans* to P. The link to the energy analysis is straightforward: if N is farther away, it donates less to the metal, so the metal is less stable.

The last factor is steric hindrance. If, as previously mentioned, steric hindrance has almost no impact on the elimination barrier, it increases the destabilization induced by the coordination of the third ethylene molecule and slightly affects the insertion barrier. Therefore, it can be concluded that steric hindrance creates synergic and cumulative effects favoring the elimination of 1-butene to the detriment of chain growth. Finally, though each of these three effects is quite small, the combination of these effects is significant.

Table 1 Agostic stabilization energy and energetic and geometric measures of the *trans* effect (see text for definitions). All energies are in kcal mol^{-1} and distances are in pm

	ΔG^{0}_{ago}	$t^{0}_{2\rightarrow 3}$	$t^{0}_{4\rightarrow 5}$	$t^{Ni-N}_{2\rightarrow 3}$	$t^{Ni-N}_{4\rightarrow 5}$
H	5.0	0.9	0.2	1.0	1.5
Me	6.0	2.1	2.0	1.1	1.4
Bz	6.8	2.2	2.3	1.5	2.9

Metallacycle mechanism

Oxidative coupling of two ethylenes

Even though the Cossee mechanism is fully able to explain and reproduce the experimental results, a possible alternative was also considered: the metallacycle mechanism. Nickelacyclopentane complexes have been identified and proposed as catalysts for the formation of dimers from ethylene [26, 54]. A paper by McKinney and al. [55] demonstrated that cyclization is symmetry forbidden for a nickel(0) bearing a C_{2v} bidentate ligand. Ring expansion of particular nickelacycle has also recently been studied [56].

As MAO can reduce the precatalyst, several oxidation states (in their most stable spin states) have been studied. For the doublet [Ni(I)/Ni(III)]$^{+}$, the activation barrier for the oxidative coupling is 38.7 kcal mol^{-1} (R = R′ = Me). For the singlet Ni(0)/Ni(II), it is 50.4 kcal mol^{-1}. As a result, the unusual Ni(II)/Ni(IV) couple, in its singlet configuration, was considered for further investigations (see [57–59] for examples of isolated Ni(IV) complexes).

The oxidative coupling constitutes the first step: complex **I** is transformed into metallacyclopentane **II** via the transition state **TSI** (Fig. 4). The activation barriers (about 20 kcal mol^{-1}) are not prohibitive and only slightly depend on the nature of the substituents. The transition state corresponds to a rotation of the two ethylene molecules. As expected, the C=C bonds are considerably elongated (computed to be 1.44–1.46 Å in the three cases). Remarkably, in **II**, the existence of a β-agostic interaction is made possible by the distortion of a regular cyclopentane and by the square pyramidal geometry of this d^6 complex.

Competition between butene elimination and further ethylene insertion

Complex **III** simply results from the coordination of an ethylene molecule and, as in the Cossee mechanism, it implies the loss of the agostic interaction. However, this coordination is stabilizing in the R = R′ = H case, while it is destabilizing in the R = R′ = Me case (Fig. 4). The latter destabilization comes from the interaction between the methyl on the phosphorus atom and the carbon linked to the metal in the square plane.

The insertion requires more energy (10 kcal mol^{-1} and 15 kcal mol^{-1}). As before, the whole insertion process is the sum of two steps. Since the first is stabilizing for the H case, the insertion is ultimately favored. In the methyl case, elimination and insertion are equally competitive (the energy of **TSII** is 28.8 kcal mol^{-1} vs. 28.9 kcal mol^{-1} for **TSIII**).

In the usual metallacycle mechanism, the elimination proceeds in two distinct steps [60]. The first consists of a classical β-elimination process, in which a hydride is transferred to the metal, with the chain remaining linked to the metal and bearing a C=C double bond at its end. This intermediate is usually a local minimum. Then, in a second step, the complex undergoes reductive elimination, giving 1-butene. In our calculations, the hydride complex is not a minimum but a first-order saddle point, the imaginary frequency corresponding to the direct transfer of the β-hydrogen to the δ carbon, which is assisted by the nickel atom. This elimination, occurring in a single step, may be related to the electron-rich nature of the metal (noting that it has not been observed for group IV catalysts).

The introduction of a bulky group onto the nitrogen group has a tremendous effect on the selectivity of the catalysis. In fact, in this case, **TSIII** lies at higher energy

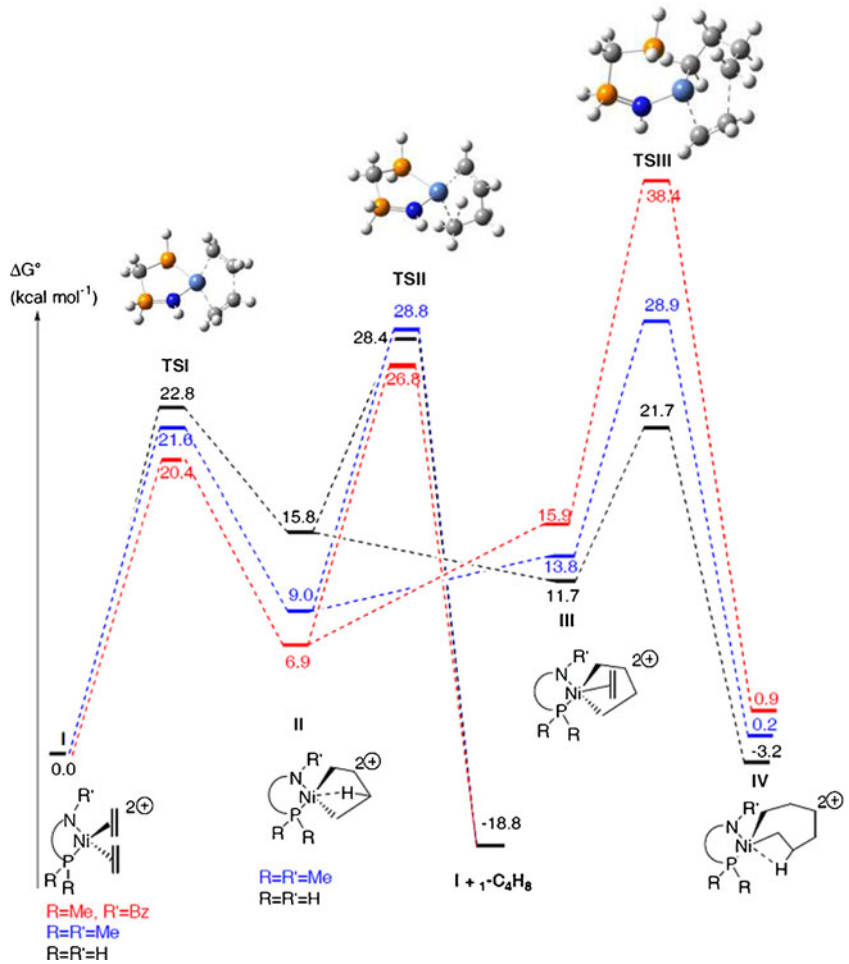

Fig. 4 Oxidative coupling, and butene elimination vs. ethylene insertion (*orange* P, *gray* C, *white* H, *dark blue* N, *light blue* Ni)

than **TSII** (11.6 kcal mol^{-1}): butene elimination is indisputably preferred, which is partly explained by the energetic cost of ethylene coordination (>9.0 kcal mol^{-1}, compared to 4.8 kcal mol^{-1} when R = R′ = Me). The insertion barrier itself also increases when going from R′ = Me (15.1 kcal mol^{-1}) to R′ = Bz (22.5 kcal mol^{-1}). Again, both components of the overall insertion process work synergistically to disfavor chain growth when steric hindrance increases. On the contrary, the elimination barrier is not affected (it is about 19 kcal mol^{-1} in both cases).

Hexene elimination

Exactly the same situation that was observed for the Cossee mechanism was computed here too: the ethylene complex is higher in energy than the transition state for elimination (Fig. 5). Therefore, as also seen for butene elimination, the hexene is released in one step; the hydride complex is the transition state.

More insights into the determination of the active species

Modeling the activation

As both mechanisms are consistent with experimental data, the key to distinguishing between them is the activation process, starting from the dibromide complex (which was experimentally found to be in the triplet state; note that such a change in spin from the precursor to the active species has already been reported [61, 62]). As the real MAO structure is still unknown, we chose to explore the potential energy surface of the activation using trimethylaluminium as model for the real MAO. Indeed, experimentally, the oligomer distributions obtained when using $AlMe_3$ as the activator are very close to those obtained with MAO. Such similarities prompted us to assume that the active species created by $AlMe_3$ and MAO are the same. Also, given the size of the system, we restricted our study to the H case. In this context, it is also worth mentioning that some studies of activation paths have already been reported in the literature [63, 64].

The first step is the creation of a Lewis-type adduct with two $AlMe_3$ equivalents (complexes **B1** and **B3**, Fig. 6), requiring about 8 kcal mol^{-1}, whatever the spin state. **B1** can undergo a small transformation that consists of a rotation of the Al–Br bond that shifts bromine outside the metallic coordination sphere (**B1b**) and can be considered the first debromination. It should also be noted that a second debromination can occur from **B1b**, leading to a dimethyl complex that cannot be active as an oligomerization catalyst, as the square plane is saturated. As all these intermediates are higher in energy than **B3**, their formation is disfavored. Analogously, a similar debromination is possible from this latter complex, but it gives **B3b**, which is also less stable than **B3**. No double debromination product from **B3** has been identified.

In conclusion, no change in spin is expected, and the unmethylated complex **B3** was computed to be the predominant species by far. As a consequence, the only viable way to make it evolve is to proceed to an elimination of $[AlMe_3Br]^-$.

There are two possibilities, depending on which of the aluminium fragments is eliminated: we chose the one with the longest Ni–Br distance. Strikingly, the triplet and the singlet products have almost the same Gibbs energy (Fig. 7). In **C1**, a methyl is linked to the metal. Thus, if **C1** is the species with the lowest activation barrier to formation, the

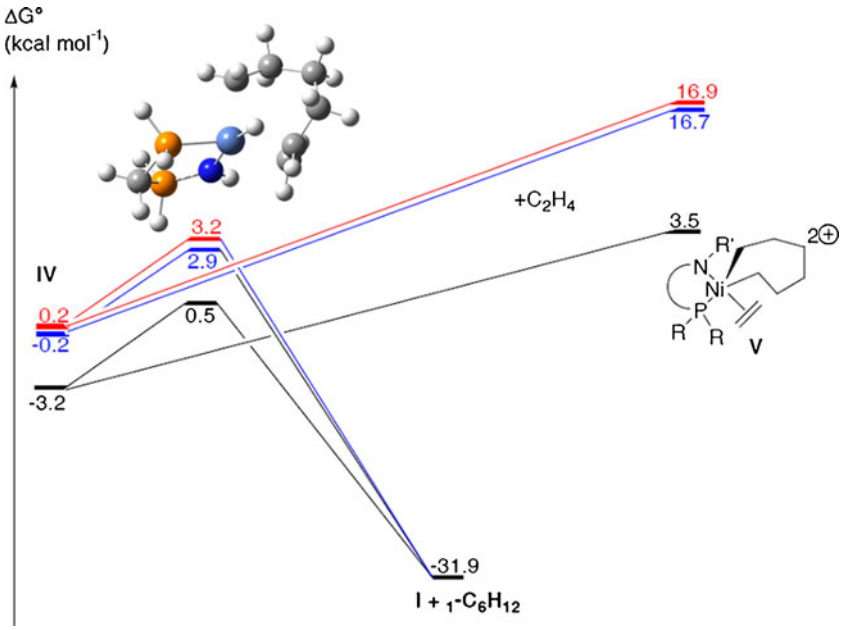

Fig. 5 Competition between second ring expansion and hexene elimination (*orange* P, *gray* C, *white* H, *dark blue* N, and *light blue* Ni)

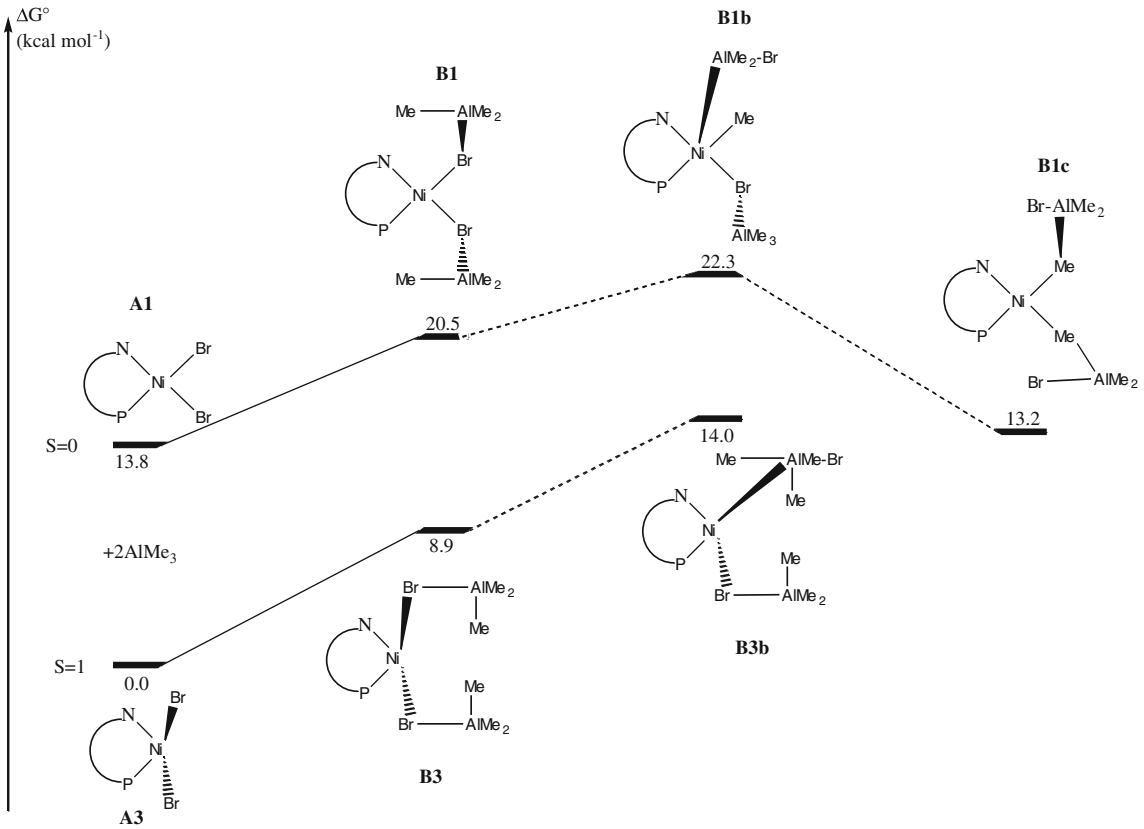

Fig. 6 Coordination of two equivalents of triethylaluminum to the precatalyst

Cossee mechanism will be preponderant. The triplet complex **C3** can give **C3b**, in which a methyl group has been transferred to the metal. However, this transformation is not thermodynamically favored. Therefore, in the absence of ethylene, **C3** is the most stable triplet complex, and the only one that can lead to either Cossee or metallacycle mechanisms

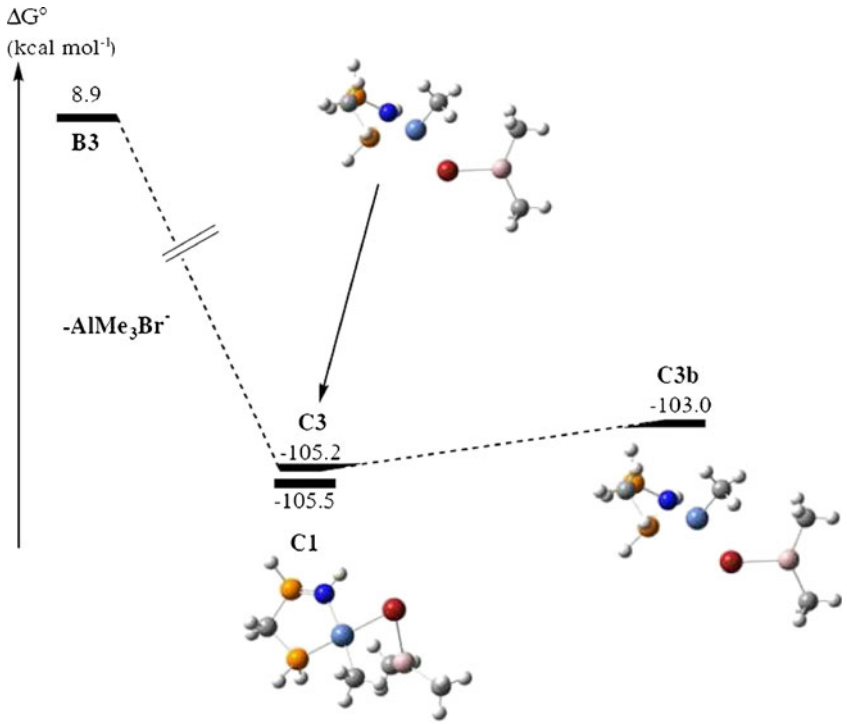

Fig. 7 Elimination of the $[AlMe_3Br]^-$ moiety (*orange* P, *gray* C, *white* H, *dark blue* N, *light blue* Ni, *pink* Al, *red* Br)

when ethylene coordinates. If we can show that **C3** mainly induces the Cossee mechanism, we will have proven that in either case (triplet or singlet), it is this mechanism that dominates. We will not then need to determine whether it is **C1** or **C3** that is most easily formed from **B3**.

When ethylene coordinates to the nickel center, **D3** can be obtained, where two methyl groups are transferred to the metal. This transfer is promoted by the significant elongation of the corresponding Al–C bonds: to 2.04 Å in both cases (whereas the value for the third—noninteracting—methyl group is 1.95 Å). Accordingly, these two methyl groups can be considered agostic, and exhibit unusual angles (NiAlC = 63° and BrAlC = 117°). In order to quantify the energy that is required to capture the methyl with the shortest Ni–C distance, a relaxed energy scan on this coordinate was performed. It appears that the surface is very flat and that the transfer requires less than 4.5 kcal mol^{-1}, so that the Cossee mechanism will be active, whatever the spin state. It should also be noted that the methyl group finally comes in *trans* to nitrogen. After ethylene insertion and propene release, we thus obtain a hydride *trans* to nitrogen, **1a1**, consistent with our previous findings.

Conclusions

In this paper, we utilized DFT calculations to investigate the reaction mechanism for the dimerization of ethylene using three model (P,N) nickel(II) catalysts. For the two mechanisms envisaged (Cossee and metallacycle), singlet nickel (II) complexes are the active species, and the dimer is always predominant for the bulkiest model catalyst.

These results prompted us to examine the activation process and propose that the Cossee mechanism is the predominant one for this catalytic transformation when MAO is used as the activator.

Our calculations also allow us to propose some guidelines for the creation of nickel(II) complexes with high catalytic performance. It was found that the elimination barrier was almost independent of the substituents chosen. On the contrary, the whole insertion process is disfavored when the steric hindrance is increased. It is important to note that this insertion is the sum of two steps: the insertion itself and the previous coordination of an ethylene molecule. In the Cossee mechanism, this coordination occurs at the less favorable site, namely *trans* to phosphorus for the third insertion, which explains the observed selectivity. This *trans* effect was related to the increase in the Ni–N bond length.

Finally, three important ligand properties were found to be fundamental:

1) Bifunctionality. There must be two electronically different binding sites on the ligand to disfavor the coordination of the third ethylene.
2) A sterically hindered substituent on the nitrogen atom. While improving stabilization through a β-agostic interaction, it again suppresses chain elongation and thus promotes butene elimination.
3) Relative flexibility. The ligand must permit all of the important geometrical modifications that allow the stabilization of the metal center along the reaction pathway. However, the selectivity for butene was shown to be enhanced when the ligand was able to stabilize a planar conformation. A delicate balance between flexibility and rigidity is therefore needed.

For completeness, it is worth noting that we studied the influence of the computational protocol in [65] and the possible quantitative prediction of ΔG^0_{pref} in [66].

Acknowledgments The CNRS (Centre National de la Recherche Scientifique), the Ecole Polytechnique, the Ecole Nationale Supérieure de Chimie, and the IDRIS (Institut du Développement et des Ressources en Informatique; for computer time, projects no. 171616 and 72115) are thanked for supporting this work. This paper is dedicated to the memory of Pascal Le Floch, who initiated the collaborative work between our groups.

References

1. Vogt D (1996) In: Cornils B, Hermann WA (eds) Applied homogeneous catalysis with organometallic compounds, vol 1. Wiley, Weinheim, pp 245–258
2. Lappin GR, Sauer JD (1989) Alpha-olefins applications handbook. Marcel Dekker, Berkeley
3. Kaminsky W, Arndt M (1996) In: Cornils B, Hermann WA (eds) Applied homogeneous catalysis with organometallic compounds, vol 1. Wiley, Weinheim, pp 220–236
4. Köhn RD, Haufe M, Kociok-Kohn G, Grimm S, Wasserscheid P, Keim W (2000) Selective trimerization of α-olefins with triazacyclohexane complexes of chromium as catalysts. Angew Chem Int Ed 39:4337–4339
5. Carter A, Cohen SA, Cooley NA, Murphy A, Scutt J, Wass DF (2002) High activity ethylene trimerisation catalysts based on diphosphine ligands. Chem Commun 858–859
6. Bollmann A, Blann K, Dixon JT, Hess FM, Killian E, Maumela H, McGuinness DS, Morgan DH, Neveling A, Otto S, Overett M, Slawin AMZ, Wasserscheid P, Kuhlmann S (2004) Ethylene tetramerization: a new route to produce 1-octene in exceptionally high selectivities. J Am Chem Soc 126:14712–14713
7. McGuinness DS, Wasserscheid P, Morgan DH, Dixon JT (2005) Ethylene trimerization with mixed-donor ligand (N,P,S) chromium complexes: effect of ligand structure on activity and selectivity. Organometallics 24:552–556
8. Agapie T, Day MW, Henling LM, Labinger JA, Bercaw JE (2006) A chromium-diphosphine system for catalytic ethylene trimerization: synthetic and structural studies of chromium complexes with a nitrogen-bridged diphosphine ligand with *ortho*-methoxyaryl substituents. Organometallics 25:2733–2742
9. Elowe PR, McCann C, Pringle PG, Spitzmesser SK, Bercaw JE (2006) Nitrogen-linked diphosphine ligands with ethers attached to nitrogen for chromium-catalyzed ethylene tri- and tetramerizations. Organometallics 25:5255–5260

10. Jabri A, Crewdson P, Gambarotta S, Korobkoc I, Duchateau R (2006) Isolation of a cationic chromium(II) species in a catalytic system for ethylene tri- and tetramerization. Organometallics 25:715–718
11. Schofer SJ, Day MW, Henling LM, Labinger JA, Bercaw JE (2006) Ethylene trimerization catalysts based on chromium complexes with a nitrogen-bridged diphosphine ligand having *ortho*-methoxyaryl or *ortho*-thiomethoxy substituents: well-defined catalyst precursors and investigations of the mechanism. Organometallics 25:2743–2749
12. McGuinness DS, Rucklidge AJ, Tooze RP, Slawin AMZ (2007) Cocatalyst influence in selective oligomerization: effect on activity, catalyst stability, and 1-hexene/1-octene selectivity in the ethylene trimerization and tetramerization reaction. Organometallics 26:2561–2569
13. Svejda SA, Brookhart M (1999) Ethylene oligomerization and propylene dimerization using cationic (α-diimine)nickel(II) catalysts. Organometallics 18:65–74
14. Tellman KP, Gibson VC, White AJP, Williams DJ (2005) Selective dimerization/oligomerization of α-olefins by cobalt bis(imino)pyridine catalysts stabilized by trifluoromethyl substituents: group 9 metal catalysts with productivities matching those of iron systems. Organometallics 24:280–286
15. Speiser F, Braunstein P, Saussine L (2005) Catalytic ethylene dimerization and oligomerization: recent developments with nickel complexes containing P, N-chelating ligands. Acc Chem Res 38:784–793
16. Lejeune M, Semeril D, Jeunesse C, Matt D, Peruch F, Lutz PL, Ricard L (2004) Diphosphines with expandable bite angles: highly active ethylene dimerisation catalysts based on upper rim, distally diphosphinated calix[4]arenes. Chem Eur J 10:5354–5360
17. Ajellal N, Kuhn MCA, Boff ADG, Horner M, Thomas CM, Carpentier JF, Casagrande OL (2006) Nickel complexes based on tridentate pyrazolyl ligands for highly efficient dimerization of ethylene to 1-butene. Organometallics 25:1213–1216
18. Buchard A, Auffrant A, Klemps C, Vu-Do L, Boubekeur L, Le Goff XF, Le Floch P (2007) Highly efficient P–N nickel(II) complexes for the dimerisation of ethylene. Chem Commun 1502–1504
19. Boubekeur L, Ricard L, Mézailles N, Le Floch P (2005) Synthesis of new mixed phosphineiminophosphorane bidentate ligands and their coordination to group 10 metal centers. Organometallics 24:1065–1074
20. Boubekeur L, Ricard L, Mézailles N, Demange M, Auffrant A, Le Floch P (2006) Nitrogen-assisted ortho lithiation: one-pot synthesis of new classes of bidentate and tetradentate mixed P~N ligands. Organometallics 25:3091–3094
21. Koch W, Holthausen MC (2000) A chemist's guide to density functional theory of atoms and molecules. Wiley-VCH, Weinheim
22. Parr RG, Yang W (1989) Density functional theory of atoms and molecules. Oxford University Press, New York
23. Ziegler T (1995) The 1994 Alcan Award Lecture: density functional theory as a practical tool in studies of organometallic energetics and kinetics. Beating the heavy metal blues with DFT. Can J Chem 73:743–761
24. Morokuma K, Musaev DG (2008) Computational modeling for homogeneous and enzymatic catalysis: a knowledge-base for designing efficient catalysts. Wiley-VCH, Weinheim
25. Fan L, Krzywicki A, Somogyvari A, Ziegler T (1994) Density functional study of ethylene dimerization by (Acetylacetonato)nickel hydride Inorg Chem 33:5287–5294
26. Bernardi F, Bottoni A, Rossi I (1998) A DFT investigation of ethylene dimerization catalyzed by Ni(0) complexes. J Am Chem Soc 120:7770–7775
27. Shiotsuki M, White PS, Brookhart M, Templeton JL (2007) Mechanistic studies of platinum(II)-catalyzed ethylene dimerization: determination of barriers to migratory insertion in diimine Pt(II) hydrido ethylene and ethyl ethylene intermediates. J Am Chem Soc 129:4058–4067
28. Cossee P (1964) Ziegler–Natta catalysis. I. Mechanism of polymerization of α-olefins with Ziegler–Natta catalysts. J Catal 3:80–88
29. Fink G, Mülhaupt R, Brintzinger H (1995) Ziegler catalysts. Springer, Berlin
30. Tempel DJ, Johnson LK, Huff RL, White PS, Brookhart M (2000) Mechanistic studies of Pd(II): α-diimine-catalyzed olefin polymerizations. J Am Chem Soc 122:6686–6700
31. Leatherman MD, Svejda SA, Johnson LK, Brookhart M (2003) Mechanistic studies of nickel(II) alkyl agostic cations and alkyl ethylene complexes: investigations of chain propagation and isomerization in (α-diimine)Ni(II)-catalyzed ethylene polymerization. J Am Chem Soc 125:3068–3081
32. Liu WJ, Brookhart M (2004) Mechanistic studies of palladium(II)-α-diimine-catalyzed polymerizations of *cis*- and *trans*-2-butenes. Organometallics 23:6099–6107
33. Bianchini C, Giambastiani G, Rios IG, Mantovani G, Meli A, Segarra AM (2006) Ethylene oligomerization, homopolymerization and copolymerization by iron and cobalt catalysts with 2,6-(bis-organylimino)pyridyl ligands. Coord Chem Rev 250:1391–1418
34. Emrich R, Heinemann O, Jolly PW, Kruger C, Verhovnik GPJ (1997) The role of metallacycles in the chromium-catalyzed trimerization of ethylene. Organometallics 16:1511–1513
35. Overett MJ, Blann K, Bollmann A, Dixon JT, Haasbroek D, Killian E, Maumela H, McGuinness DS, Morgan DH (2005) Mechanistic investigations of the ethylene tetramerisation reaction. J Am Chem Soc 127:10723–10730
36. Frisch MJ et al. (2003) Gaussian 03, revision B.05. Gaussian, Inc., Pittsburgh
37. Becke AD (1993) Density–functional thermochemistry. III. The role of exact exchange. J Chem Phys 98:5648–5652
38. Poater A, Solans-Monfort X, Clot E, Coperet E, Eisenstein O (2007) Understanding d^0-olefin metathesis catalysts: which metal, which ligands? J Am Chem Soc 129:8207–8216
39. Guihaumé J, Halbert S, Eisenstein O, Perutz RN (2012) Hydrofluoroarylation of alkynes with ni catalysts. C–H activation via ligand-to-ligand hydrogen transfer, an alternative to oxidative addition. Organometallics 31:1300–1314
40. Hay PJ, Wadt WR (1985) Ab initio effective core potentials for molecular calculations. Potentials for the transition metal atoms Sc to Hg. J Chem Phys 82:270–283
41. Cho HG, Cheong BS (2009) Agostic interaction of the smallest zirconium methylidene hydride: reproduction of the distorted structure experimentally observed in matrix infrared spectra. Bull Korean Chem Soc 30:479–481
42. Vidal I, Melchor S, Alkorta I, Elguero J, Sundberg MR, Dobado JA (2006) On the existence of α-agostic bonds: bonding analyses of titanium alkyl complexes. Organometallics 25:5638–5647
43. Virkkunen V, Pietilä LO, Sundholm F (2003) DFT investigation of the regiospecifity of a model catalyst site for propene polymerisation. Polymer 44:3133–3139
44. Fukui K (1981) The path of chemical reactions: the IRC approach. Acc Chem Res 14:363–368
45. Gonzalez C, Schlegel HB (1990) Reaction path following in mass-weighted internal coordinates. J Phys Chem 94:5523–5527
46. Liang L-C, Chien PS, Lee P-Y (2008) Phosphorus and olefin substituent effects on the insertion chemistry of nickel(II) hydride complexes containing amido diphosphine ligands. Organometallics 27:3082–3093
47. Chen EYX, Marks TJ (2000) Cocatalysts for metal-catalyzed olefin polymerization: activators, activation processes, and structure−activity relationships. Chem Rev 100:1391–1434

48. Sinn H, Kaminsky W (1980) Ziegler–Natta catalysis. Adv Organomet Chem 18:99–149
49. Johnson LK, Killian CM, Brookhart M (1995) New Pd(II)- and Ni(II)-based catalysts for polymerization of ethylene and α-olefins. J Am Chem Soc 117:6414–6415
50. Musaev DG, Froese RDJ, Svensson M, Morokuma K (1997) A density functional study of the mechanism of the diimine−nickel-catalyzed ethylene polymerization reaction. J Am Chem Soc 119:367–374
51. Margl P, Deng LQ, Ziegler T (1999) A unified view of ethylene polymerization by d^0 and d^0f^n transition metals. 3. Termination of the growing polymer chain. J Am Chem Soc 121:154–162
52. Talarico G, Budzelaar PHM (2006) A second transition state for chain transfer to monomer in olefin polymerization promoted by group 4 metal catalysts. J Am Chem Soc 128:4524–4525
53. Tellmann KF, Humphries MJ, Rzepa HS, Gibson VC (2004) Experimental and computational study of β-H transfer between cobalt(I) alkyl complexes and 1-alkenes. Organometallics 23:5503–5513
54. Grubbs RH, Miyashita A (1978) Metallacyclopentanes as catalysts for the linear and cyclodimerization of olefins. J Am Chem Soc 100:7416–7418
55. McKinney RJ, Thorn DL, Hoffmann R, Stockis A (1981) Nickelacyclopentane complexes. A theoretical investigation. J Am Chem Soc 103:2595–2603
56. Hsiao J, Su M-D (2008) Theoretical characterizations of the ring expansion of a metallacyclopropane to a metallacyclopentane. Organometallics 27:4139–4146
57. Klein H-F, Bickelhaupt A, Lemke M, Jung T, Röhr C (1995) Synthesis and structure of octahedral nickel(IV) complexes containing two chelating acylphenolato ligands. Chem Lett 24:467–468
58. Patra AK, Mukherjee R (1999) Direct detection of aqueous diazene: its UV spectrum and concerted dismutation. Inorg Chem 38:1388–1393
59. Dimitrov V, Linden A (2003) A pseudotetrahedral, high-oxidation-state organonickel compound: synthesis and structure of bromotris(1-norbornyl)nickel(IV). Angew Chem Int Ed 42:2631–2633
60. Blok ANJ, Budzelaar PHM, Gal AW (2003) Mechanism of ethene trimerization at an *ansa*-(arene)(cyclopentadienyl) titanium fragment. Organometallics 22:2564–2570
61. Brückner A, Jabor JK, McConnell AEC, Webb PB (2008) Monitoring structure and valence state of chromium sites during catalyst formation and ethylene oligomerization by in situ EPR spectroscopy. Organometallics 27:3849–3856
62. Bianchini C, Gatteschi D, Giambastiani G, Guerrero Rios I, Ienco A, Laschi F, Mealli C, Meli A, Sorace L, Toti A, Vizza F (2007) Electronic influence of the thienyl sulfur atom on the oligomerization of ethylene by cobalt(II) 6-(thienyl)-2-(imino)pyridine catalysis. Organometallics 26:726–739
63. Zurek E, Ziegler T (2002) Toward the identification of dormant and active species in MAO (methylaluminoxane)-activated, dimethylzirconocene-catalyzed olefin polymerization. Organometallics 21:83–92
64. Janse van Rensburg W, van den Berg J-A, Steynberg PJ (2007) Role of MAO in chromium-catalyzed ethylene tri- and tetramerization: a DFT study. Organometallics 26:1000–1013
65. Tognetti V, Le Floch P, Adamo C (2010) How the choice of a computational model could rule the chemical interpretation: the Ni(II) catalyzed ethylene dimerization as a case study. J Comput Chem 31:1053–1062
66. Tognetti V, Fayet G, Adamo C (2010) Can molecular quantum descriptors predict the butene selectivity in nickel(II) catalyzed ethylene dimerization? A QSPR study. Int J Quantum Chem 110:540–548